Comparison of two different grades of carbon steel reinforcement in the synthetic concrete pore solution

Ahmed Kareem Abdulameer, **Saheb Mohammed Mahdi**

Materials Engineering Department, Mustansiriayah University, Baghdad, Iraq.

Abstract

The research aims to investigate the impact of carbon steel grade on corrosion resistance in a synthetic concrete pore (SCP) solution. For this investigation, two grades of carbon steel as specified by ASTM A615-16 were selected, GR-60 (420MPa) and GR-80 (550MPa), respectively. In this study, the open circuit potential (OCP) and Tafel polarization plots were utilized and conducted at a temperature of 24 °C. In addition, the metallographic inspection was also performed for both grades. The electrochemical corrosion behavior of the two steel grades is assessed in the same (SCP) solution. The results showed that the open circuit potential of GR-80 of about (-375 mV) is nobler than GR-60 of (-385 mV), indicating the passive layer of GR-80 has better quality. In addition, the cathodic slopes of the Tafel plot for both grades are approximately equal (0.111 V/decade) for GR-80 and (0.107 V/decade) for GR-60. However, the anodic slope of GR60 (0.257 V/decade) is relatively higher than GR-80 (0.222 V/decade), indicating more iron (F^{++}) ions dissolution for GR-60. Consequently, the findings that were obtained via the application of the mixed potential theory and Faraday's law showed that the corrosion resistance of GR-80 (0.305 μm/y) in the same environment is more than that of GR-60 (0.353 μm/y) as a result of chemical changes and variances in steel's matrix microstructural characteristics that effect on the protective oxide layer formed on the steel surface.

Keywords: Tafel plot, carbon steel corrosion, mixed potential theory, synthetic concrete pore solution.

1. Introduction

Reinforced concrete may provide structures and buildings with a service life of many decades when properly planned, built, and maintained. Reinforcing steel is well protected from corrosion by concrete. Because of the very alkaline environment in concrete, a thin protective oxide layer (passive) of stable and tightly adhering will form on the steel reinforcing surface, protecting it from corrosion. Furthermore, properly proportioned, compacted, and cured concrete will have a low penetrability, which reduces the ingress of species that cause corrosion through the aqueous phase [1].

Rebar corrosion is the term used to describe the natural rusting process when reinforced steel bars are placed in concrete structures. In other words, corrosion of steel-reinforced concrete is the degradation of metal (such as steel reinforcement) by electrochemical, chemical, or electrolytic reactions on the steel surface within the concrete environment. It develops when the concrete ages [2]. Even with the advanced technologies created to protect steel from corrosion, including paint systems and proactive

electrochemical approaches (e.g., cathodic protection), time-consuming maintenance procedures are unavoidable, and their costs may be extremely expensive. Steel encased in concrete may potentially create a long-lasting, low-maintenance building material. Except under extreme climatic situations, experience with numerous buildings has shown that this is the case. Despite the theory and a good track record in many projects, steel corrosion in concrete has become a significant durability issue in moderate and severe climatic situations in the last three decades. However, in the early time, there were mainly concerns with the concrete's performance, such as resistance to sulfate attack, which is frequent in maritime constructions; it seems that the main overall durability issue now is steel corrosion in concrete [3].

Steel corrosion is a significant issue for civil engineers. Steel's corrosion susceptibility is recognized to be affected by a variety of factors, including its composition, micro-structure, production, and environment. Continuous attempts have been undertaken to enhance the characteristic of current reinforcement steel and as well as to produce better ones that are stronger, harder, and more corrosion-resistant. Further, specific rebar steels, including epoxy-coated steel, galvanized steel, and stainless steel, are frequently utilized in particular cases [4]. As a result, various processing techniques and heat treatments may enhance microstructural changes in the steel, increasing corrosion resistance without reducing strength or other properties. Microcell galvanic corrosion occurs when the localized potentials on the rebar surface vary due to different phases and morphologies in the steel microstructure [5].

Many research works for the corrosion evolution of carbon steel rebar in concrete have been published. For instance, Bautista et al. [6] studied the corrosion behavior of carbon steel rebars type B-500-SD (according to EN 10080) with a diameter of 12mm and 30mm high test specimens. They compare the outer rebar surface of martensite case with ferritic-perlitic in the core. They showed that, in solution testing, the corrosion current of martensite is somewhat greater than that of ferrite-perlite, and their corrosion potential is nearly equivalent. Sarraf et al. [7] studied the effects of the grain size of low-carbon steel on its electrochemical activity in a synthetic concrete pore solution. Three types of specimens were used: as-received, coarse (with grains about twice the size of as-received steel), and fine (with grains about half the size of as-received specimens). The samples were immersed in a solution with and without chloride addition (3% wt. NaCl). The specimens' corrosion behavior was measured using several electrochemical measuring methods. The findings indicated that fine specimens passivated first, followed by coarse and as-received samples. When compared to the as-received specimens, the mass loss of the fine and coarse specimens was reduced by 72% and 91%, respectively. Kumar P. et al. [8] investigated the impact of rebar steel microstructures (coarse, fine, very fine ferrite-pearlite, martensite, and tempered martensite) on corrosion behavior in modeled concrete pore solution. The employed rebar steel has chemical composition of (0.25C, 0.19Si, 0.75Mn, 0.024P, 0.04S, 0.02Cr, 0.02Ni, 0.01Nb, 0.05Ta, and 98.5Fe). The samples immersed in simulated (CPS) containing [0.1M $Ca(OH)_2$, 0.1M NaOH, 0.2M KOH, and 0.003M $CaSO_4.2H_2O$]. Three-electrode cell, (EIS), dynamic polarization tests, corrosion current density, and Raman spectroscopy were performed in this study. Their results reached, the corrosion rate of the test sample as follows: very fine ferrite-pearlite and martensite is (0.004 mm/y), fine ferrite-pearlite is (0.005 mm/y), coarse ferrite-pearlite is (0.006 mm/y), and tempered steel is (0.007mm/y).

Jiang et al. [9] investigate the galvanic corrosion in modeled concrete pore solutions of corrosion-resistant Cr10Mo1 (CR) rebar and low carbon reinforcement bars (LC). They employ three different solutions, one low alkaline with pH values of (9.0, 11.3, and 13.6). Each solution was supplemented with chloride at a 5 mol/L concentration. Tafel polarization and open circuit potential (OCP) was performed in this work. The open-circuit potentials of CR were around (-270 mV), and LC was around (-360 mV) at a pH value of 9.0. The steady open-circuit values were around -260 and -330mV, respectively, at pH 11. For CR and LC, the open-circuit potentials at pH 13.6 were roughly -210 and -256 mV. The findings demonstrated that the difference between LC and CR E_{corr} values reduced when pH increased, as did the driving force for galvanic corrosion between the two electrodes. At the same pH, the i_{corr} of LC was higher than that of CR, and CR displayed greater corrosion resistance than LC. When raising the pH, the i_{corr} for both CR and LC was lowered, showing that both CR and LC displayed increased corrosion resistance. Shanmugapriya et al. [10] compare the corrosion resistance of mild steel submerged in a synthetic cement pore solution (SCPS) and well water. They utilized the major components of the concrete pore solution, which are saturated calcium hydroxide $Ca(OH)_2$, sodium hydroxide (NaOH), and potassium hydroxide (KOH), with a pH of (13.5). Polarization curve and open-circuit potential were employed in this investigation. They indicate that the i_{corr} was (1.835×10^{-6} A/cm^2) and the E_{corr} was (-547 mV) when the samples were submerged in well water. The corrosion current was (1.573×10^{-6} A/cm^2) when mild steel was submerged in SCP solution, which displaced the E_{corr} to the anodic side (-525 mV). This displacement shows that the anodic areas of the metal

surface have been protected from corrosion by forming a more protective layer during the process of passivation when the steel is immersed in SCPS compared to well water. Dey et al. [11] investigated four rebars to see how different alloying components and micro-structural constituents affected corrosion behavior. This research compares the corrosion-resistant stainless steel, Fe-600, plain, and galvanized steel submerged in two distinct solutions of 1% HCl and 3.5% NaCl. Electrochemical measurements of open circuit potential (OCP) and Tafel plot were used in this study. The results showed that the OCP of stainless steel, Fe-600, plain, and galvanized steel in 1% HCL are (−0.588, −0.565, −0.572, and −1.056 V, respectively) and in 3.5% NaCl are (−0.527, −0.779, −0.666, and −1.131, respectively). Also, the corrosion rate of stainless steel, Fe-600, plain, and galvanized steel in 1% HCL are (14.847, 7.225, 8.390, and 104.09 mm/year, respectively) and in 3.5% NaCl are (1.545, 0.930, 0.864, and 2.929 mm/year, respectively).

H. Torbati-Sarraf and A. Poursaee [12] used a synthetic concrete pore solution to examine how phase distribution and steel microstructure affect corrosion onset and chloride threshold value. Cyclic heat treatment and Normalizing were utilized to change the grain size, MnS, and pearlite morphology of standard reinforcing carbon steel. Cyclic voltammetry and electrochemical impedance spectroscopy. Cyclic voltammetry and electrochemical impedance spectroscopy (EIS) were used to compare microstructure oxidation with non-treated steel specimens. The results showed the Normalizing coarsening MnS inclusions and pearlite phase, while the cyclic-heat treatment refined them. In addition, the reference steel has a chloride threshold value of 1.2M. In contrast, Normalized steel reduced the chloride threshold value to 0.8 M, and cyclic heat treatment improved the corrosion initiation resistance to about 1.5 M. P. K. Katiyar et al. [13] employed steels with different amounts of carbon (0.7, 0.43, 0.17, and 0.002% C) having fully pearlite, ferrite-pearlite, and ferrite microstructures were chosen to find out how carbon steel corrodes in a 3.5% NaCl solution with free oxygen. Methods including dynamic polarization, electrochemical impedance, and linear polarization were used. The corrosion rate obtained from the various carbon steels was found to continue rising from (0.044 mm/y) for steel containing (0.002% C) with ferrite microstructure to (0.17 mm/y) for steel containing (0.17%) with fully pearlite microstructure. Because of the influences of the pearlite percentage, cementite-to-ferrite area ratio, and interlamellar spacing, the corrosion rate gradually rises when steel's carbon content increases from low to medium to high.

Consequently, much research compares different steel types, such as galvanizing steel, plain steel, chromium steel, etc., or different steel phases, such as Ferrite, Pearlite, Martensite, etc., or uses solutions with varying values of pH or chloride ions contaminations. However, the effect of the same steel type with different grades on corrosion behavior has been little studied or not focused on sufficiently. Using the Tafel electrochemical technique and the Echem Analyst program, the authors of this research investigate the influence of carbon steel grade on the corrosion resistance of reinforcing steel bars in a solution that simulates concrete conditions.

2. Experimental work

2.1. Materials and solutions

Two Different kinds of carbon steel rebar grades, grade 60 with a minimum yield strength of (420 MPa) and grade 80 with a minimum yield strength of (550 MPa), according to ASTM A615 standard specification [14].

Both rebar grades were machined and tapped to prepare cylindrical samples of 9.5 mm (± 0.1 mm) in diameter and 12.7 mm (± 0.1 mm) in height to investigate corrosion behavior. All samples were wet ground with 240-grit silicon carbide paper and then wet polished using 600-grit silicon carbide paper to eliminate the coarse scratches. After that, the samples were washed with acetone and de-ionized water before being dried in the open-air [15]. The elemental composition of the two-steel grade rebar used in this investigation is listed in Table 1, using spark atomic emission Spectrometry and was conducted according to ASTM E415 [16]. In addition, the metallographic inspection was performed for both steel grades and shown in Figure 1.

Table 1. Results of elemental analysis for carbon steel rebar (expressed as mass percent, %).

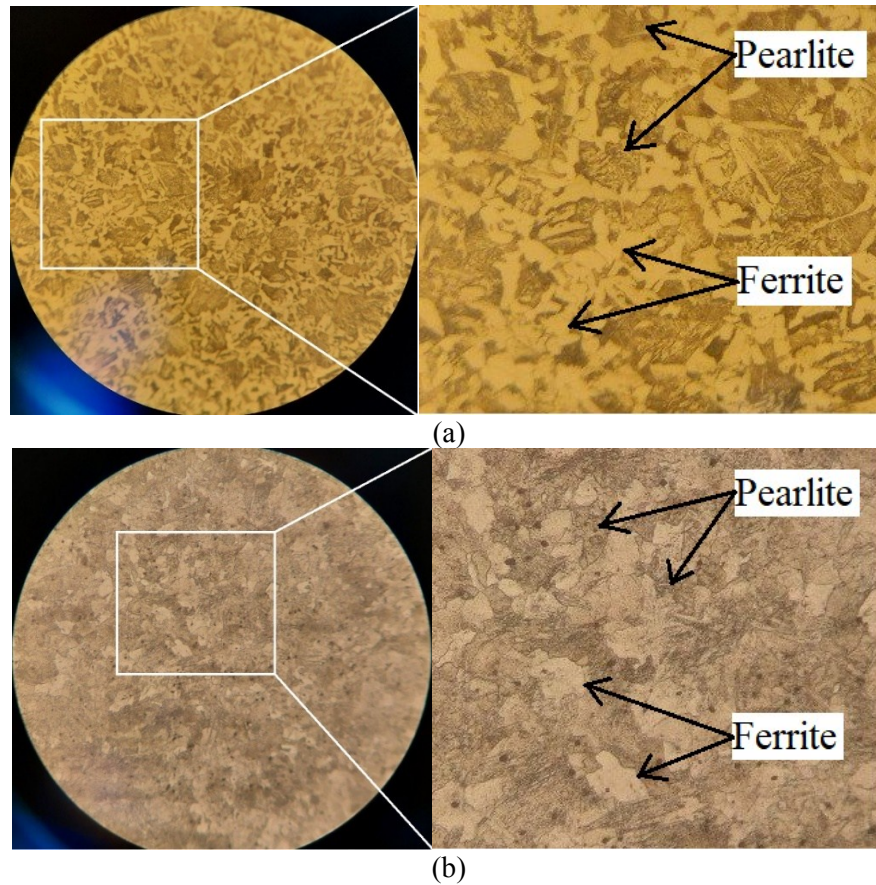|	Fe	C	Si	Mn	Cr	Mo	Ni	Al	Co	Cu
Grade 60	98.2	0.201	0,346	0,360	0,0215	0,0156	0,1200	0,0133	0,0958	0,0369
Grade 80	98,3	0,145	0,130	0,847	0,0595	< 0,004	0,128	0,0116	0,0834	0,0557

Figure 1. Metallographic test with magnification of 500X: (a) for grade 60, (b) for grade 60.

The synthetic concrete pore solution (SCPs) was prepared by dissolving 0.01mol/L $Ca(OH)_2$, 0.1mol/L NaOH, 0.3mol/L KOH, and 0.002mol/L $CaSO_4.2H_2O$. The solution was stirred for one hour regularly, and the measured pH value was (≈13) [17].

2.2. Electrochemical Measurements
As demonstrated in Figure 2, a three-electrode cell system was used to perform Tafel polarization experiments.
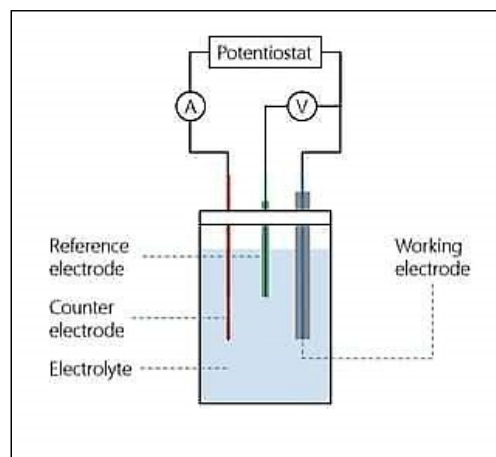

Figure 2. Three-electrode cell configuration.

The working electrode (WE) was a steel specimen, the reference electrode (RE) was a saturated calomel electrode, and the counter electrode (CE) was a graphite electrode [15]. The samples were immersed in the SCPs for a sufficient period (approximately 12 hours) to allow the OCP to stabilize. After stabilization, the

open circuit potential (E_{oc}) was determined, and the samples were polarized in the (-250 to +250) mV/SCE range with regard to the OCP [18]. At room temperature (25 ±1), the scanning rate was 0.125 mV/s [18], and the specimens' corrosion current densities (i_{corr}) were determined using the Tafel extrapolation method, illustrated in Figure 3.
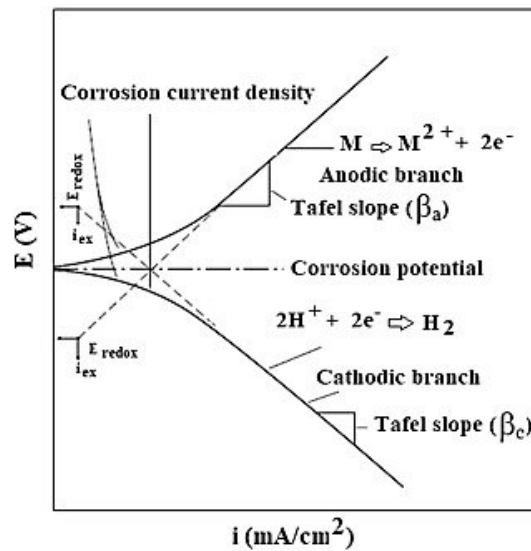

Figure 3. Typical Tafel extrapolation plot [19].

The results were analyzed using the Echem Analyst program to calculate the corrosion rates. The Butler-Volmer Eq. (1) is used in the software to describe the relationship between the current and potential (kinetic model) in a mixed potential mechanism [20]. I_{corr}, E_{oc}, βa, and βcare the four variables that may be changed in the program. The minimization algorithm is rather difficult to understand. It provides several estimations for the four parameters' values.

$$I=I_a+I_c=I_{corr}(e^{(2.3(E-Eoc)/\beta a)}-e^{(-2.3(E-Eoc)/\beta c)}) \tag{1}$$

Where, I = cell current (A), I_a = anodic current (A), I_c = cathodic current (A), I_{CORR} = corrosion current (A), βa = anodic Tafel constant (V/decade), βc = cathodic Tafel constant (V/decade), E = applied potential (V), E_{oc} = corrosion potential (V).

After each estimate, the "fitness of the estimate" is assessed by Echem Analyst program. The corrosion rates were determined using Eq. (2) below [21, 22].

$$\text{Corrosion rate (mm/year)} = i_{corr} \text{ X K X EW} / \rho \tag{2}$$

Where, i_{corr} = corrosion current density (A/cm^2), K = constant (0.00327), EW = iron equivalent weight (27.92), ρ = steel density (7.86 g/cm^3).

3. Results and discussion
Figure 4 illustrates how the open circuit potential of two different steel grades (GR-60 and GR-80) changes over time when exposed to a concrete's simulated pore solution.
With time, the OCP values of all samples altered in a more positive direction before stabilizing, which was due to the development of the passive film of (Fe_3O_4 and Fe_2O_3), according to the pH value of the solution, OCP, and Pourbaix diagram, Figure 5, for iron water [23]. Dehghanian [24] also reported a more negative potential at the first hour of immersion then the OCP shifted to a positive direction (passivity). The GR-60 sample had a slightly more negative OCP value than the GR-80 sample, possibly due to their differing chemical composition, since GR-60 has less purity, lower chromium content, and higher carbon content than GR-60, according to a Table 1, which affects on microstructural properties of the passive layer produced on the surface of the steel. This behavior matches the previously reported findings [25, 26].

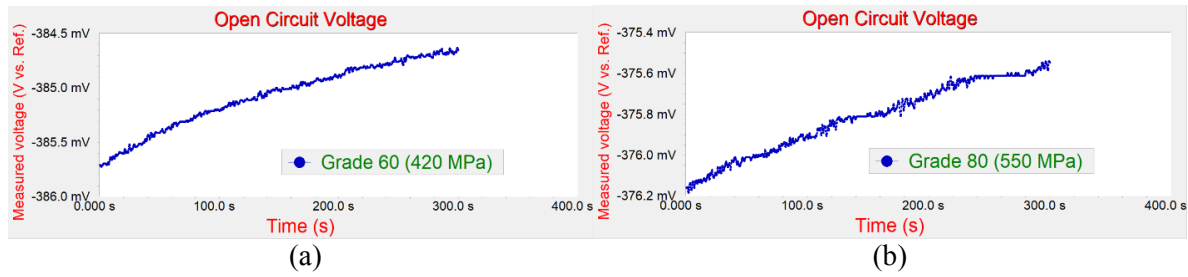(a)   (b)

Figure 4. Open circuit potential measurement: (a) for grade 60, (b) for grade 80.
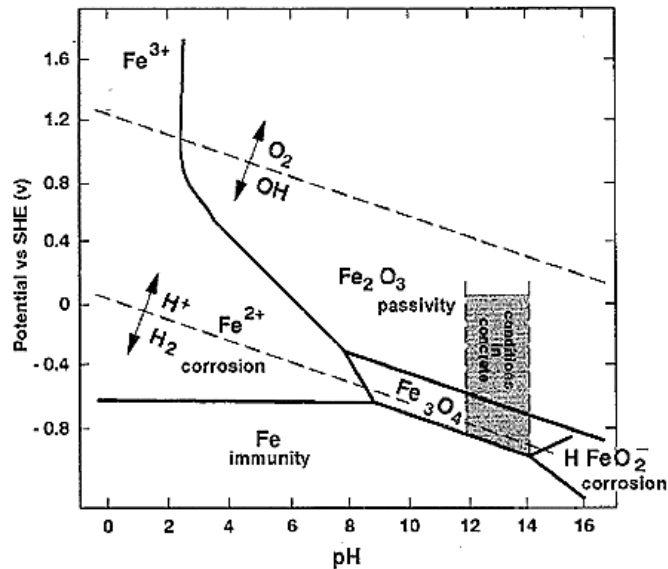

Figure 5. Potential-pH (Pourbaix) diagram for iron-water [23].

Figure 5 illustrates the polarization curves resulting from the Tafel test conducted for steel samples of varying grades submerged in the same SCP solution. The Tafel behavior is seen in the small region where the potential and logarithm of the anodic current are linearly proportional. The two curves indicate the anodic and cathodic reactions are activation controlled, and concentration polarization has no effect on the Tafel's behavior. Iron (steel) oxidation, reaction (3), and oxygen reduction, reaction (4), in the SCP solution, seems to be the anodic and cathodic reaction, respectively [27].

$$Fe \rightarrow Fe^{2+} + 2e^- \tag{3}$$

$$1/2 O_2 + H_2O + 2e^- \rightarrow 2OH^- \tag{4}$$

As shown in Figure 6, for the two grades, the anodic branch slopes (βa) are consistently greater than the cathodic branch slopes (βc). This observation indicates that the anodic process is more restricted, and the i_{corr} is more influenced by the anodic half-reaction than the cathodic reaction. The Tafel extrapolation method is used to calculate the specimen corrosion rates.

Table 2 lists important electrochemical parameters determined by polarization tests. It shows the corrosion rates are higher for steel GR-60, while steel GR-80 has lower corrosion rates in the same solution. This contrast may be attributed to a lower carbon content of GR-80; thus, less fraction of the pearlite phase is present, which is more susceptible to corrosion. In addition, although GR-80 has lower carbon content, it has higher tensile strength; this contrast can be attributed to the relatively smaller grain size, as shown in Figure 1. However, the smaller grain size has a higher activity to oxidate and form a barrier oxide layer between the metal surface and the SCP solution, thus enhances the corrosion resistance. Kumar P. et al. [8] also showed that carbon steel with a smaller grain size has higher corrosion resistance than coarser grains.
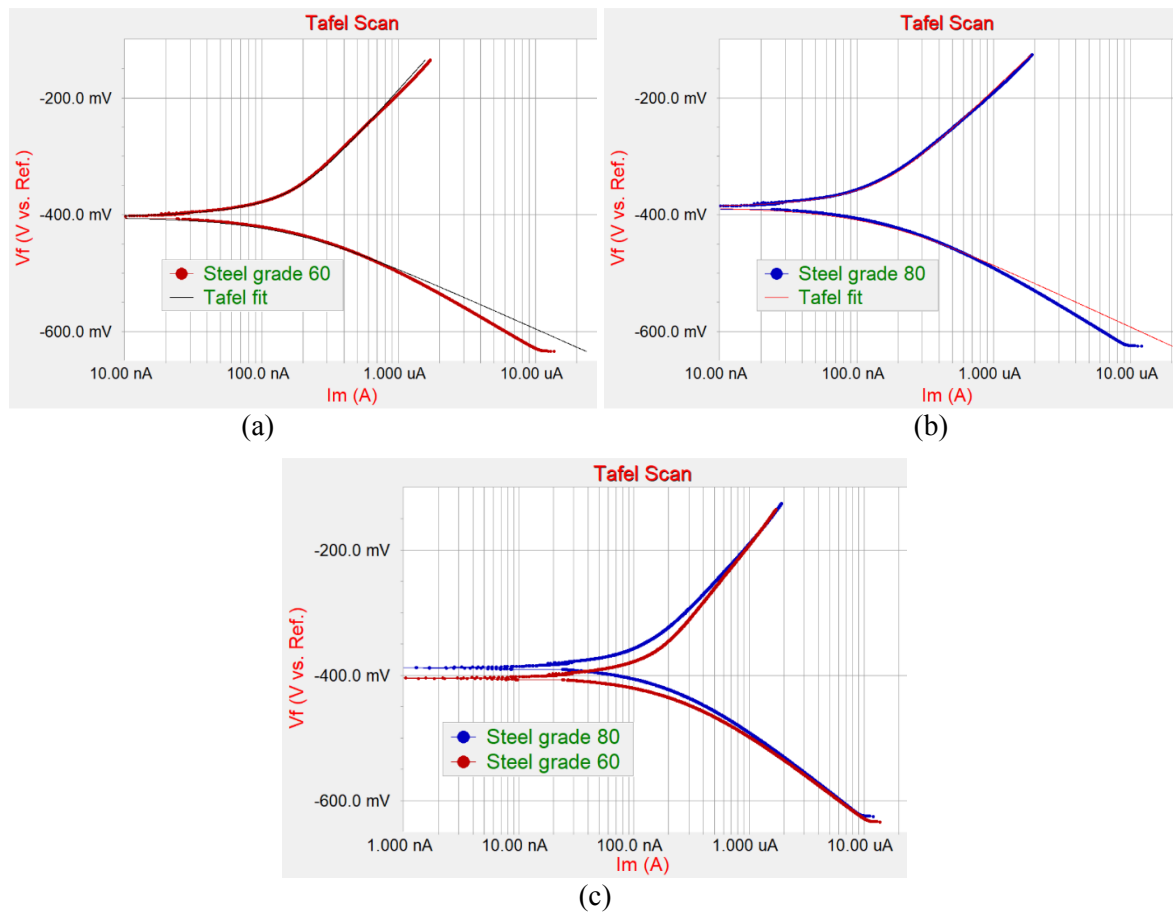
(a)

(b)

(c)

Figure 6. Tafel polarization curves; a) for steel grade 60, b) for steel grade 80, and c) comparison of grade 60 and 80 curves.

Table 2. Electrochemical parameters obtained by Tafel tests.

	Grade 60	Grade 80
OCP (mV)	-384.6	-375.5
Anodic slope (V/decade)	0.2571	0.2218
Cathodic slope (V/decade)	0.1067	0.111
i_{corr} (nA)	146	126
E_{corr} (mV)	-404	-387
Corrosion rate (µm/year)	0.3535	0.3054

The surface morphology of the specimens was inspected using an optical microscope after the polarization test. Both steel grades showed uniform corrosion (micro-corrosion) without pitting corrosion (macro-corrosion), as indicated in Figure 7. Also, GR-60 has more inclusions (darker spots) within the steel matrix than grade 80, which represents weak sites in the protective oxide layer.
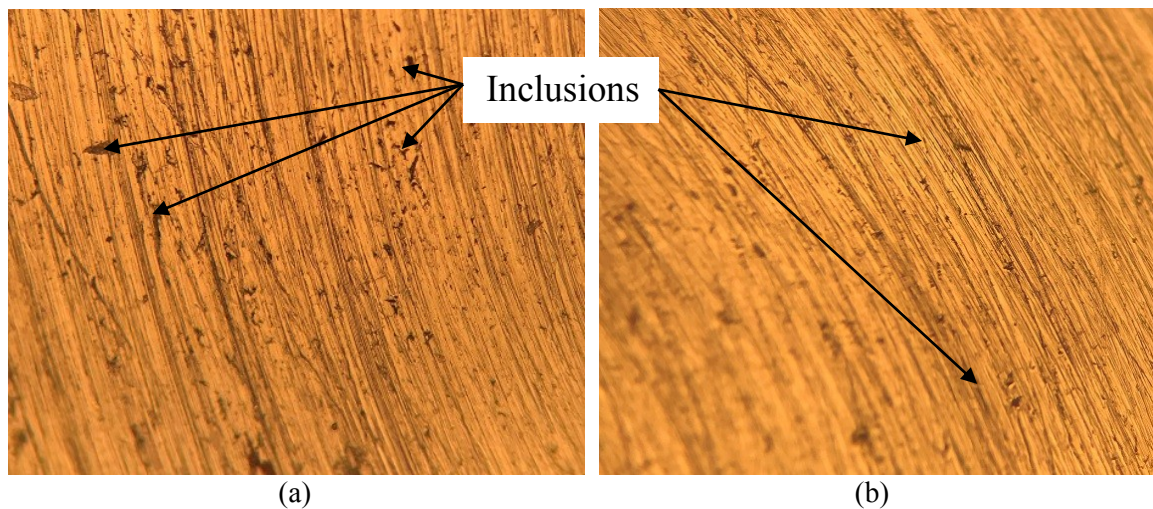
(a)   (b)

Figure 7. Optical microscope image with magnification (200X), a) for steel grade 60 and b) for steel grade 80.

4. Conclusions

This work studies the effect of carbon steel grade on reinforcing bar corrosion behavior in simulated concrete pore solution. And the iportant findings are:

- The OCP value of steel GR-60 was (-384.6 mV) slightly more negative than the GR-80 (-375.5 mV), indicating that the GR-60 is more active. These OCP variances can be attributed to the quality of the passive or barrier layer formed on the steel surface of about a few nanometer thicknesses in alkaline environments.
- The rebar steel's chemical composition and grain size affect the corrosion rate. In addition, the corrosion rates of steel GR-60 (0.353 μm/y) in the same solution are higher than GR-80 (0.305 μm/y), indicating lower uniform corrosion resistance. Also, the two grades showed uniform or micro-corrosion during the electrochemical tests without any pitting corrosion indication.
- Galvanic corrosion may be developed when both grades are used in the same construction due to the steel composition and structure differences.
- The two grades are close to each other in mechanical properties according to ASTM A615; other grades of minimum yield strength, such as 280MPa and 690MPa, may show higher differences in corrosion behaviors.

Conflict of interest

The authors state that publishing this work has no conflict of interest.

References

[1] B. Cherry and W. Green, Corrosion and Protection of Reinforced Concrete. CRC Press, 2021.
[2] A. R. Nayak and M. Dominic, "Corrosion of reinforced concrete: A Review," International Research Journal of Engineering and Technology (IRJET), vol. 08, no. 06, 2021.
[3] A. Bentur, S. Diamond, and Neal Berke, Steel corrosion in concrete: fundamentals and civil engineering practice. Taylor & Francis eLibrary, 2005.
[4] F. Lollini, M. Carsana, M. Gastaldi, and E. Redaelli, "Corrosion behaviour of stainless steel reinforcement in concrete," Corrosion Reviews, vol. 37, no. 1, pp. 3-19, 2019, doi: 10.1515/corrrev-2017-0088.
[5] D. Clover, B. Kinsella, B. Pejcic, and R. De Marco, "The influence of microstructure on the corrosion rate of various carbon steels," Journal of applied electrochemistry, vol. 35, no. 2, pp. 139-149, 2005, doi: 10.1007/s10800-004-6207-7.

[6]   A. Bautista, J. C. Pomares, M. d. l. N. González, and F. Velasco, "Influence of the microstructure of TMT reinforcing bars on their corrosion behavior in concrete with chlorides," Construction and Building Materials, vol. 229, p. 116899, 2019, doi: 10.1016/j.conbuildmat.2019.116899.

[7]   H. Torbati-Sarraf and A. Poursaee, "Corrosion improvement of carbon steel in concrete environment through modification of steel microstructure," J. Mater. Civ. Eng, vol. 31, no. 5, p. 04019042, 2019.

[8]   P. K. Katiyar, P. K. Behera, S. Misra, and K. Mondal, "Comparative corrosion behavior of five different microstructures of rebar steels in simulated concrete pore solution with and without chloride addition," Journal of Materials Engineering and Performance, vol. 28, no. 10, pp. 6275-6286, 2019.

[9]   J. Jiang, H.-y. Chu, Y. Liu, D. Wang, D. Guo, and W. Sun, "Galvanic corrosion of duplex corrosion-resistant steel rebars under carbonated concrete conditions," RSC advances, vol. 8, no. 30, pp. 16626-16635, 2018, doi: 10.1039/C8RA03320J.

[10]   S. Shanmugapriya, P. Prabhakar, and S. Rajendran, "Corrosion resistance property of mild steel in simulated concrete pore solution prepared in well water by using an aqueous extract of turmeric," Materials Today: Proceedings, vol. 5, no. 2, pp. 8789-8795, 2018, doi: 10.1016/j.matpr.2017.12.307.

[11]   I. Dey, P. Manna, M. Yadav, N. K. Tewary, J. K. Saha, and S. K. Ghosh, "Study on the Perspective of Mechanical Properties and Corrosion Behaviour of Stainless Steel, Plain and TMT Rebars," in Stainless Steels, 2021: IntechOpen, doi: 10.5772/intechopen.101388.

[12]   H. Torbati-Sarraf and A. Poursaee, "The influence of phase distribution and microstructure of the carbon steel on its chloride threshold value in a simulated concrete pore solution," Construction and Building Materials, vol. 259, p. 119784, 2020.

[13]   P. K. Katiyar, S. Misra, and K. Mondal, "Corrosion behavior of annealed steels with different carbon contents (0.002, 0.17, 0.43 and 0.7% C) in freely aerated 3.5% NaCl solution," Journal of Materials Engineering and Performance, vol. 28, no. 7, pp. 4041-4052, 2019.

[14]   ASTM A615/A615M-15a, "Standard Specification for Deformed and Plain Carbon-Steel Bars for Concrete Reinforcement," in ASTM, USA, ed, 2015.

[15]   ASTM G5-14, "Standard Reference Test Method for Making Potentiodynamic Anodic Polarization Measurements," in ASTM International: West Conshohocken, PA, USA, ed, 2014.

[16]   Standard Test Method for Analysis of Carbon and Low-Alloy Steel by Spark Atomic Emission Spectrometry, ASTM E415 − 17, 2017.

[17]   Z. Dong and A. Poursaee, "Corrosion behavior of coupled active and passive reinforcing steels in simulated concrete pore solution," Construction and Building Materials, vol. 240, p. 117955, 2020.

[18]   P. S. Umoren, D. Kavaz, and S. A. Umoren, "Corrosion Inhibition Evaluation of Chitosan–CuO Nanocomposite for Carbon Steel in 5% HCl Solution and Effect of KI Addition," Sustainability, vol. 14, no. 13, p. 7981, 2022.

[19]   A. Hossain, M. A. Gafur, F. Gulshan, and A. S. W. Kurny, "Electrochemical investigation of the corrosion behavior of heat treated Al-6Si-0.5 Mg-xCu (x= 0, 0.5 and 1) alloys," Journal of Electrochemical Science and Engineering, vol. 5, no. 1, pp. 1-8, 2015.

[20]   P. P. Deshpande and D. Sazou, Corrosion Protection of Metals by Intrinsically Conducting Polymers. CRC Press, 2016.

[21]   ASTM G102-89, "Standard practice for calculation of corrosion rates and related information from electrochemical measurements," in ASTM International: West Conshohocken, PA, USA, ed, 2010.

[22]   T. Bremner, K. Hover, R. Poston, J. Broomfield, T. Joseph, R. Price, K. Clear, M. Khan, D. Reddy, and J. Clifton, "ACI 222R-01 protection of metals in concrete against corrosion," American Concrete Institute: Farmington Hills, MI, USA, 2001.

[23]   W. Green, F. Collins, and M. Forsyth, "Up-to-date review of aspects of steel reinforcement corrosion in concrete," Corrosion and materials, vol. 43, no. 3, pp. 64-76, 2018.

[24]   C. Dehghanian, "Study of surface irregularity on corrosion of steel in alkaline media," Cement and concrete research, vol. 33, no. 12, pp. 1963-1966, 2003, doi: 10.1016/S0008-8846(03)00215-1.

[25]   D. Song, J. Jiang, W. Sun, H. Ma, J. Zhang, Z. Cheng, J. Jiang, and Z. Ai, "Effect of chromium micro-alloying on the corrosion behavior of a low-carbon steel rebar in simulated concrete pore solutions," Journal of Wuhan University of Technology-Mater. Sci. Ed., vol. 32, no. 6, pp. 1453-1463, 2017, doi: 10.1007/s11595-017-1768-6.

[26]   R. Hussain, J. Singh, A. Alhozaimy, A. Al-Negheimish, C. Bhattacharya, R. Pathania, and D. Singh, "Effect of Reinforcing Bar Microstructure on Passive Film Exposed to Simulated Concrete Pore Solution," Aci materials journal, vol. 115, no. 2, 2018.

[27]   M. G. Richardson, Fundamentals of durable reinforced concrete. CRC Press, 2002.

Ahmed Kareem Abdulameer E-mail address: ebma042@uomustansiriyah.edu.iq
Phone Number: 07702592825

Saheb Mohammed Mahdi E-mail address: saheb.m.mahdi@uomustansiriyah.edu.iq
Phone Number: 07707279486